



## Bizarre parosteal osteochondromatous proliferation: 16 Cases with a focus on histologic variability

Margaret Cocks<sup>a,1</sup>, Elizabeth Helmke<sup>a,1</sup>, Carolyn A. Meyers<sup>a</sup>, Laura Fayad<sup>b</sup>, Edward McCarthy<sup>a</sup>, Aaron W. James<sup>a,\*</sup>

<sup>a</sup> Department of Pathology, Johns Hopkins University, United States

<sup>b</sup> Department of Radiology, Johns Hopkins University, United States



### ARTICLE INFO

#### Keywords:

BPOP  
Bone tumor  
Cartilage tumor  
Osteochondroma  
Surface bone tumor

### ABSTRACT

Bizarre parosteal osteochondromatous proliferation (BPOP) is a benign bone and cartilage forming tumor occurring on the surface of bones, predominantly on the hands and feet. A defining feature of BPOP is the purplish-blue mineralization of cartilaginous tissue, known as ‘blue bone.’ Here, we report on an institutional series of 16 cases of BPOP, including radiographic, histologic, and histomorphometric features. All tumors were composed of some element of bone, cartilage, fibrous tissue and ‘blue bone,’ though the amount of each tissue sub-type varied widely. Some cases showed focal ‘blue bone’ only, however this was a defining feature in all cases.

### 1. Introduction

Bizarre parosteal osteochondromatous proliferation (BPOP, also called Nora’s Lesion) is a benign tumor that occurs predominantly in the tubular bones of the hands and feet including the phalanges, metacarpal and metatarsal bones.<sup>1,2</sup> BPOP may occasionally arise on the long bones. BPOP has been found in patients ranging in age from 8 to 73 years, though the tumor is most common during the second and third decades.<sup>1</sup> No sex predilection has been identified. Tumors generally are less than 3 cm and are painless. A history of trauma is elicited in about 10% of cases. Recurrence is common and may be seen in up to 50% of cases, likely due to partial excision. On radiographic imaging, BPOP is most often described as a well-circumscribed, radiodense mass arising adjacent to the cortical surface.<sup>1,2</sup> Medullary continuity between the lesion and native bone is not seen.

Grossly, the appearance of BPOP is that of a bone and cartilage containing exophytic mass without continuity with the underlying bone medullary cavity. BPOP tumors may be received intact or as a morse-lized tissue aggregate. Histologically, BPOP has a ‘disorganized’ architectural appearance on low magnification, with aggregates of cartilage, new bone, and fibrous tissue. In some cases, a cartilaginous cap may be seen. BPOP is often marked by hypercellular, reactive and somewhat atypical cartilage and fibrous stroma, which invokes concern over the lesion’s malignant potential. Marked nuclear hyperchromasia or atypical mitotic figures are not seen. A distinguishing feature of BPOP is blue-staining osteocartilaginous tissue, known as ‘blue bone.’

As BPOP is a rare and frequently misdiagnosed tumor, we reviewed our institutional case files for all observed cases. Sixteen cases of BPOP were identified with radiographic and histologic correlates, which shed new light on both the common features and variability within this unusual entity.

### 2. Methods

#### 2.1. Identification of bizarre parosteal osteochondromatous proliferation samples

Sixteen cases diagnosed as BPOP were identified in our surgical pathology archives (dated 1994–2016). IRB approval was obtained, which included a waiver of informed consent for this retrospective case series. The clinical, radiographic, and histologic data of the sixteen cases were compiled. Two pathologists independently verified the diagnoses.

#### 2.2. Image acquisition

Radiographic images were obtained from institutional case files, imaged using a 12-megapixel digital camera with an f/2.2 aperture (Fig. 1). Histological slides were digitally scanned using an Aperio automated slide scanner, and one representative image of each sample was taken. Additional images for publication were taken using the NDP view2 software at 40 x and 100 x magnification (Fig. 2).

\* Corresponding author at: Department of Pathology, Johns Hopkins University, Ross Research Building, Room 524A, 720 Rutland Avenue, Baltimore, MD, United States.

E-mail address: [awjames@jhmi.edu](mailto:awjames@jhmi.edu) (A.W. James).

<sup>1</sup> The authors share equally in the work presented herein.



**Fig. 1.** Representative radiographic images of bizarre parosteal osteochondromatous proliferation. All were taken of the hands except for D, which is of the toes. (A) Dorsal multilobular radiodensity of the fourth distal phalanx with surrounding soft tissue prominence that has no apparent communication to the underlying bone marrow. (B) Parosteal radiodense mass adjacent to the middle phalanx of the third digit, appears to be a surface lesion. (C) Soft tissue mass with radiodensity distal to the distal phalanx. (D) Soft tissue mass with peripheral radiodensity that is associated with the distal phalanx, probably with periosteal reaction. Appearance of this lesion is less mature than in the prior examples. (E) Dorsal soft tissue lesion with internal radiodensity at the level of the interphalangeal joint of the thumb. Note similarity to radiograph in part A. (F) Radiodense mass at the proximal aspect of the proximal phalanx of the digit. From this view, possible attachment to the adjacent bone cortex cannot be excluded. (G) Volar surface lesion along the distal phalanx with peripheral radiodensity. (H) Large radiodense mass with smooth external border along the proximal metacarpal of the long finger with unclear relationship to the underlying bone.

### 2.3. Analysis of bizarre parosteal osteochondromatous proliferation samples

After digital slide imaging at 40 $\times$  magnification, the percentage tissue composition of each sample was quantified using Adobe Photoshop based histomorphometry. Quantified areas of tissues included bone, cartilage, fibrous tissue and ‘blue bone,’ examined using two independent techniques. First, each tissue type with a distinct hue on H&E staining was quantified using the “magic wand tool” in Photoshop, selecting and counting pixels of a similar hue. Blue bone, cartilage, and bone tissue were quantified in this manner, and divided by the total number of pixels in the image to yield the percentage composition of each tissue type. Fibrous tissue was quantified using the “lasso” selection tool, as variability in hue precluded use of the magic wand tool (Supplemental Fig. 1). Again, the composition of fibrous tissue was calculated by dividing pixels of fibrous tissue by total pixel number in the image. Percentages were rounded to the nearest 5%. Tissue composition for each sample was compiled into graphs using GraphPad Prism (Fig. 3).

### 2.4. Statistical methods

Percent composition of tissue type for each sample was determined by histomorphometric analysis of representative 40 $\times$  images. Percentages summing to 100% for each sample are presented in a bar graph in Fig. 3A. Scatterplots in Fig. 3B–E organize the data by tissue type. Dots in the scatterplots represent individual samples, while

sample mean and SEM are indicated by crosshairs and whiskers. Values are accurate to within 5%.

## 3. Results

### 3.1. Patient demographics

16 cases of BPOP were identified for inclusion. Five of the patients were female (5/16, 31%). Patients’ ages ranged from 18 to 79, with six cases occurring between 20 and 40 years of age. 14 cases were located on the hands (14/16, 88%), 2 on the feet (2/16, 13%), 13/16 (81%) in the phalanges and 3/16 (19%) in the metacarpals. Of the tumors in the phalanges, 2/12 (17%) were located on the proximal phalanx, 7/12 (58%) on the distal phalanx and 3/12 (25%) on the middle phalanx. One case on the phalanx did not include specific location information (Supplemental Table 1).

### 3.2. Radiographic appearance

Available radiologic images are shown in Fig. 1. A radiodense mass was noted on or adjacent to the bone surface in all cases. Location was variable, with some lesions identified at the proximal phalanx (Fig. 1F), middle phalanx (Fig. 1B), distal phalanx (Fig. 1C,D,F), volar surface (Fig. 1G) or dorsal surface (Fig. 1E). No apparent communication to the underlying medullary cavity was identified in any instance. There was also a range of maturity of lesion, from predominant soft tissue swelling



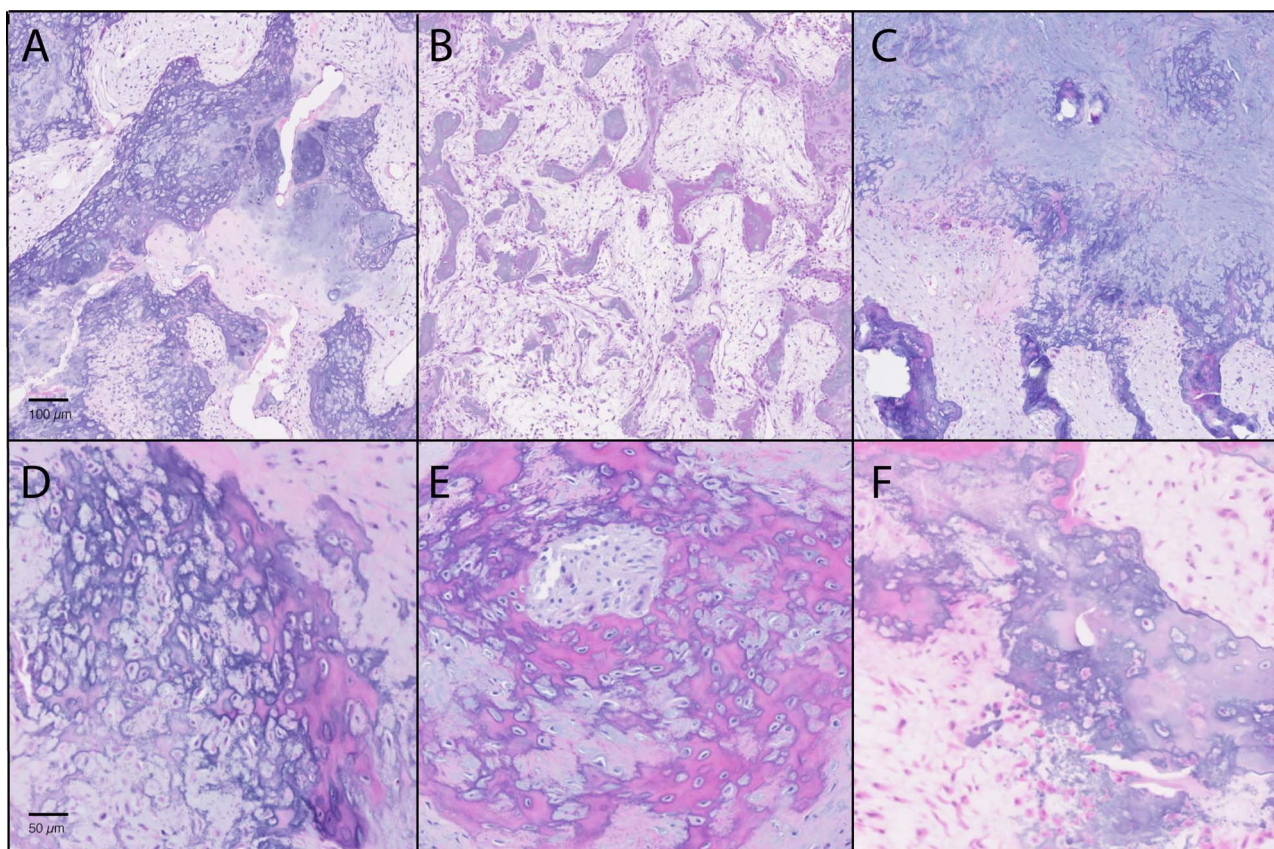


**Fig. 2.** Representative histologic images of bizarre parosteal osteochondromatous proliferation. H&E staining was used on tissue samples. A–C were obtained at 40 × magnification; D–F were obtained at 100 × magnification. (A) Representative image of BPOP with abundant ‘blue bone’. (B) Representative image of BPOP with prominent fibrous tissue. (C) Representative images of BPOP with prominent cartilage. In all cases a mixture of fibrous, osseous, and cartilaginous tissue is seen. (D–F) At high magnification, a variable appearance of ‘blue bone’ is seen between samples.

and wispy, cloud-like radiodensity (Fig. 1D) to more well demarcated radiodensities (Fig. 1H). Peripheral radiodensity was seen in some cases (Fig. 1D,F,H), while others were more radiopaque internally (Fig. 1A,E).

### 3.3. Histological appearance

All samples exhibited typical histologic features of BPOP, including some amount of cartilaginous, osseous, and fibrous tissue (Fig. 2). On low magnification, the relative proportions of tissue types varied widely. Some lesions were characterized by a preponderance of ‘blue bone’ (Fig. 2A), while others were composed of predominantly loose fibrous stroma, bone and focal blue bone (Fig. 2B). Proportion of cartilage varied widely as well, from inconspicuous (Fig. 2B) to widespread (Fig. 2C).

On higher magnification, the histologic appearance of ‘blue bone’ was also quite variable (Fig. 2D–F). The cellularity of blue bone ranged from hypercellular (Fig. 2D,E) to hypocellular and matrix-rich (Fig. 2F). In some areas, hypercellularity imparted an appearance of ‘lace-like’ osteoid (Fig. 2D). Hue of ‘blue bone’ also varied from specimen to specimen. Most had a deeply basophilic appearance (Fig. 2D), while in other specimens the overall bone appearance was eosinophilic and blended with focal areas of darker blue (Fig. 2E). In these instances, the presence of ‘blue bone’ was more easily missed on low magnification.

### 3.4. Histomorphometric analysis

Histomorphometric quantification of all images using Adobe Photoshop yielded percentages of ‘blue bone,’ bone, cartilage, and fibrous tissue in each case, as summarized in Fig. 3. Amount of ‘blue

bone’ ranged from 5 to 30% with the sample mean falling at 20% (Fig. 3B). The quantity of bone tissue varied widely between specimens, ranging from 0 to 75% with a mean of 21% (Fig. 3C). Cartilage tissue was similarly variable, ranging from 0 to 55% with mean of 23%, respectively (Fig. 3D). Amount of fibrous tissue spanned from 15 to 70% with a mean at 35% (Fig. 3E). Based on the results, BPOP exhibits a highly variable makeup and heterogeneous tissue composition. The presence of some amount of ‘blue bone’ was a consistent feature across samples.

## 4. Discussion

BPOP has several features that can raise the suspicion of malignancy, including rapid growth, high rate of recurrence, and an atypical histological appearance. Awareness of the clinical, radiographic, and histologic features of BPOP is important for avoiding a misdiagnosis. Our institutional case series highlights the variability in radiographic appearance and histologic composition seen from specimen to specimen, although several key features are constant.

In our analysis, all cases of BPOP demonstrated a ‘blue bone’ component (range of 5–30%). Meneses et al. first described ‘blue bone’ in 1993 as a “distinct blue tinctorial characteristic” most pronounced at the interface between bone and cartilage and present even after decalcification.<sup>3</sup> It was used by the researchers as a helpful feature for diagnosis. Other authors have described this unique feature as an “unusual mineralized cartilaginous matrix (‘blue bone’).”<sup>3,4</sup> (829) Varying amounts of cartilage, bone, and spindle cells alongside “an unusual form of calcified so-called ‘blue bone’” were used to raise suspicion of Nora’s lesion.<sup>5</sup> (537) Dashti et al. described it as a distinct “basophilic staining pattern” of calcified and ossified hypercellular

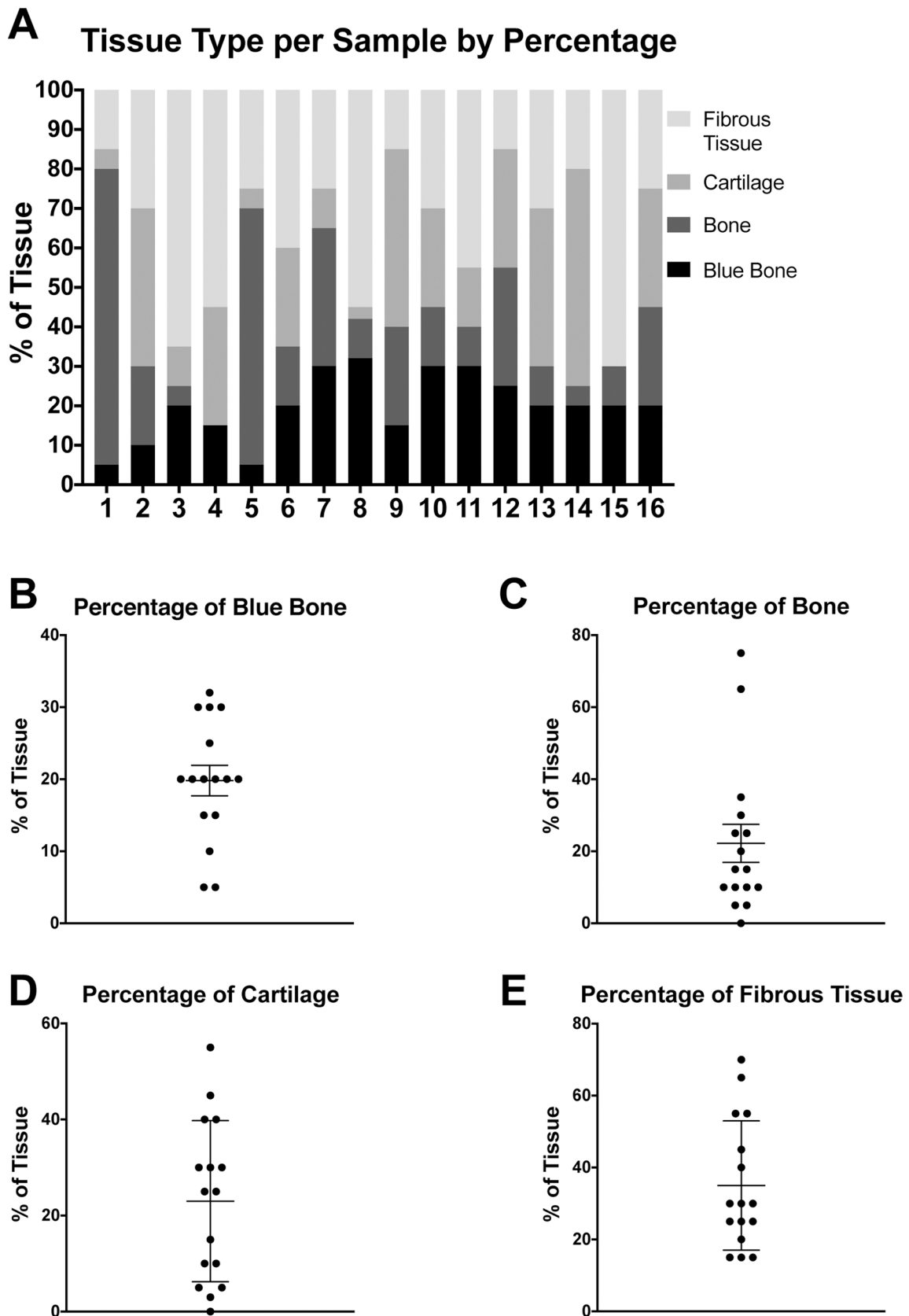


**Fig. 3.** Histomorphometric analysis of tissue composition among samples of bizarre parosteal osteochondromatous proliferation. Tissue makeup was assessed among various histologic images of BPOP, taken from each of the 16 cases included in the study. Different tissue types were established and their relative amounts were measured in each image as a percentage. **A** shows this composition for each sample. Each bar numbered 1–16 is a distinct sample corresponding to the numbered samples in Supplemental Table 1. **B–E** show the distribution of percentages in each 40× field for a given tissue type: blue bone, bone, cartilage, and fibrous tissue, respectively. Each dot represents one sample, and the horizontal lines represent the mean and standard error (SEM). (For interpretation of the references to colour in this figure legend, the reader is referred to the web version of this article.)

cartilage.<sup>6</sup> While the presence of this unique feature is often cited as part of BPOP histology, there have been no efforts to catalogue its incidence or diagnostic significance. In our series, at least some areas of ‘blue bone’ were found in every lesion examined.

While ‘blue bone’ may be used as a helpful diagnostic feature of BPOP, it is not entirely specific to the diagnosis. Other entities that demonstrate so-called ‘blue bone’ have been described, although it is likely that different findings are being discussed using the same term. Both aneurysmal bone cysts and osteoblastoma have been described as containing ‘blue bone.’<sup>7</sup> For example, in a review of 215 cases of aneurysmal bone cysts (ABCs), “blue reticulated chondroid-like material” was identified in 24/101 cases of primary ABC and in 6/114 cases of secondary ABC, with an overall incidence of 14%.<sup>8</sup>(828) One study found ‘spiculated blue bone’ in 16% of osteoblastomas.<sup>9</sup> In a more recent review of osteoblastomas, Oliveira et al. described “spiculated blue bone” as a histologic feature of atypical osteoblastoma and its presence correlated with disease recurrence.<sup>10</sup> (171) As well, it has been observed that bone infarcts are sometimes described as having a ‘blue bone’ component. Importantly, the mineral and protein composition of so-called ‘blue bone’ has not to our knowledge been characterized. In aggregate, ‘blue bone’ is a helpful descriptive term for a histologic appearance – but it is likely that different histologic findings are being lumped in to the same moniker.

The differential diagnosis for BPOP includes both benign and malignant tumors. BPOP is most commonly misdiagnosed as subungual exostosis, florid reactive periostitis and osteochondroma. Less commonly, BPOP may also be mistaken for a skeletal malignancy such as osteosarcoma or chondrosarcoma. Florid reactive periostitis (FRP) and BPOP share a similar demographic group and anatomic location. FRP has a prominent fibro-osseous component, with less prominent cartilage than BPOP. ‘Blue bone’ is not a feature of FRP. Subungual exostosis occurs in a typical location of the dorsal surface of the distal phalanx, with about 75% occurring on the great toe. On limited biopsies, distinguishing BPOP and subungual exostosis may not be possible. Osteochondromas rarely occur in the small bones of the distal extremities. Radiographic continuity with the underlying marrow cavity is a distinguishing feature of osteochondromas. Overall, the histologic appearance of osteochondroma and BPOP are dissimilar. Unless there is a history of fracture, a fibrous tissue component is typically not seen in osteochondroma, and ‘blue bone’ has not been reported.

The most common reason for referral of BPOP is to rule out a skeletal malignancy. As BPOP is a mixture of fibrous, osseous and chondroid tissue, potential diagnostic confusion is possible with high grade surface osteosarcoma, parosteal or periosteal osteosarcoma, or chondrosarcoma. Both osteosarcoma (OS)<sup>11,12</sup> and chondrosarcoma<sup>13</sup> are very rare on the hands or feet. Likewise, less common variants of OS such as periosteal and parosteal osteosarcoma involving the hands or feet are rare with only a few cases reported in the literature. For this reason, the most challenging area is to distinguish the rare BPOP of a long tubular bone from a skeletal malignancy of the bone surface. Distinguishing histologic features of each entity should be considered. Parosteal osteosarcoma demonstrates a characteristic biphasic fibro-osseous appearance, with focal cartilaginous differentiation in some cases. Periosteal osteosarcoma often has a feather-like pattern of endochondral ossification, which is distinct from the ‘blue bone’ of BPOP. Chondrosarcoma is best characterized as a permeative cartilaginous tumor. A low threshold for consultation should be used in most cases, especially for tumors in an unusual anatomic location.

The etiology of BPOP remains unclear. Given the histologic overlap with entities such as florid reactive periostitis and subungual exostosis, in the past authors have suggested that BPOP is part of a spectrum of reactive proliferative lesions. Most recently, however, research has suggested that BPOP is a clonal process. Molecular studies have shed light on potential cytogenetic abnormalities characteristic of BPOP. An

analysis of five cases of BPOP observed that t(1;17)(q32;q21), or variant translocations involving 1q32, are recurrent and unique abnormalities in BPOP.<sup>14</sup> Other independent cytogenetic analyses have supported these results. Other studies have reported separate anomalies in BPOP, suggesting that multiple chromosomal rearrangements may be seen.

Based on our observations, while the presence of ‘blue bone’ is not entirely specific for BPOP, the absence of ‘blue bone’ may be used to exclude BPOP from the differential diagnosis. The presence of ‘blue bone’ in addition to a significant fibrous component may point towards BPOP as the diagnosis. The complete clinical picture, including pathology, radiology and clinical presentation should be considered in total.

### Conflict of interests

None.

### Acknowledgements

The present work was supported by the NIH/NIAMS (K08 AR068316), the Musculoskeletal Transplant Foundation, the Orthopaedic Research and Education Foundation with funding provided by the Musculoskeletal Transplant Foundation, and Catherine and Constantinos J. Limas Research Award.

### Appendix A. Supplementary data

Supplementary data associated with this article can be found, in the online version, at <https://doi.org/10.1016/j.jor.2018.01.028>.

### References

1. Meneses MF, Unni KK, Swee RG. Bizarre parosteal osteochondromatous proliferation of bone (Nora's lesion). *Am J Surg Pathol.* 1993;17(7):691–697.
2. Yuen M, Friedman L, Orr W, Cockshott WP. Proliferative periosteal processes of phalanges: a unitary hypothesis. *Skeletal Radiol.* 1992;21(5):301–303.
3. Rybak LD, Abramovici L, Kenan S, Posner MA, Bonar F, Steiner GC. Cortico-medullary continuity in bizarre parosteal osteochondromatous proliferation mimicking osteochondroma on imaging. *Skeletal Radiol.* 2007;36(9):829–834.
4. Abramovici L, Steiner GC. Bizarre parosteal osteochondromatous proliferation (Nora's lesion): a retrospective study of 12 cases, 2 arising in long bones. *Human Pathol.* 2002;33(12):1205–1210.
5. Doganavsargil B, Argin M, Sezak M, Keceli B, Pehlivanoglu B, Oztop F. A bizarre parosteal osteochondromatous proliferation (Nora's lesion) of metatarsus, a histopathological and etiological puzzle. *Joint Bone Spine.* 2014;81(6):537–540.
6. Dashti HM, Reith JD, Schlott BJ, Lewis EL, Cohen DM, Bhattacharyya I. Bizarre parosteal osteochondromatous proliferation (Nora's Lesion) of the mandible a rare bony lesion. *Head Neck Pathol.* 2012;6(2):264–269.
7. Karkuzhali P, Bhattacharyya M, Sumitha P. Multiple soft tissue aneurysmal cysts: an occurrence after resection of primary aneurysmal bone cyst of fibula. *Indian J Orthop.* 2007;41(3):246–249.
8. Bahk WJ, Mirra JM. Differential diagnostic value of blue reticulated chondroid-like material in aneurysmal bone cysts: a classic histopathologic analysis of 215 cases. *Am J Clin Pathol.* 2015;143(6):823–829.
9. Lucas DR, Unni KK, McLeod RA, O'Connor MI, Sim FH. Osteoblastoma: clinicopathologic study of 306 cases. *Human Pathol.* 1994;25(2):117–134.
10. Oliveira CR, Mendonca BB, Camargo OP, et al. Classical osteoblastoma, atypical osteoblastoma, and osteosarcoma: a comparative study based on clinical, histological, and biological parameters. *Clinics (Sao Paulo, Brazil).* 2007;62(2):167–174.
11. Okada K, Wold LE, Beabout JW, Shives TC. Osteosarcoma of the hand: a clinicopathologic study of 12 cases. *Cancer.* 1993;72(3):719–725.
12. Mirra JM, Kameda N, Rosen G, Eckardt J. Primary osteosarcoma of toe phalanx: first documented case: review of osteosarcoma of short tubular bones. *Am J Surg Pathol.* 1988;12(4):300–307.
13. Fayad LM, Ahlawat S, Khan MS, McCarthy E. Chondrosarcomas of the hands and feet: a case series and systematic review of the literature. *Eur J Radiol.* 2015;84(10):2004–2012.
14. Nilsson M, Domanski HA, Mertens F, Mandahl N. Molecular cytogenetic characterization of recurrent translocation breakpoints in bizarre parosteal osteochondromatous proliferation (Nora's lesion). *Human Pathol.* 2004;35(9):1063–1069.